Nonlinearity 6 (1993) 1055–1066. Printed in the UK

The amplitude of periodic plane waves depends on initial conditions in a variety of λ–ω systems

Jonathan A Sherratt†
Merton College, Oxford OX1 4JD, UK
and
Centre for Mathematical Biology, Mathematical Institute, 24-29 St Giles', Oxford OX1 3LB, UK

Received 29 March 1993
Recommended by J-P Eckmann

Abstract. λ–ω systems are an important prototype for the study of reaction–diffusion equations whose kinetics possess a stable limit cycle. Here I use such systems to investigate the evolution of periodic plane waves from exponentially decaying initial data. I begin by considering the case in which $\lambda(.)$ and $\omega(.)$ are both monotonic functions. I show that in this case the reaction–diffusion solution consists of a wave front moving across the domain, with periodic plane waves behind. I show that the amplitude of these periodic plane waves is the unique solution of a simple algebraic equation. For some parameter values, the waves of this amplitude are unstable as partial differential equation solutions and, in this case, the periodic plane waves degenerate into more irregular oscillations. I go on to consider a case in which $\lambda(.)$ is a cubic polynomial, of a form so that the algebraic equation governing periodic plane wave amplitude has more than one solution. I show that it is the waves of smallest possible amplitude that appear in the reaction–diffusion solutions, and that there is a novel bifurcation in the partial differential equations as these waves appear.

PACS numbers: 0340K

1. Introduction

Systems of reaction–diffusion equations whose kinetics possess a stable limit cycle have been used to model a number of biological and chemical systems (Tyson and Murray 1989, Courtemanche and Winfree 1991, Agladze *et al* 1984), and exhibit an extremely wide variety of solution types. In particular, spiral and scroll waves (Hagan 1982, Winfree and Strogatz 1983a, b, c, 1984) spatiotemporal chaos (Kuramoto 1978, Rovinsky 1987) and periodic plane waves (Kopell and Howard 1973, Schneider 1983) have all been studied extensively. This paper is concerned with periodic plane waves, which are waves moving with constant shape and speed, that oscillate periodically in both space and time. Solutions of this type were first studied in detail by Kopell and Howard (1973), who proved the existence of a one-parameter family of periodic plane waves in a wide class of reaction–diffusion systems in which the kinetic ordinary differential equations possess a stable limit cycle. Subsequent work has focused on the existence of periodic plane waves, and their stability as partial differential equation solutions (Ermentrout 1980, Cope 1980, Maginu 1981, Kapitula 1991).

† (E-mail: jas@vax.oxford.ac.uk)

0951-7715/93/061055+12$07.50

An issue that has received very little attention in the literature is the type of initial conditions that give rise to periodic plane waves. I address this question here for a simple class of reaction–diffusion systems whose kinetics have a stable limit cycle, namely λ–ω systems. These are equations of the form

$$u_t = u_{xx} + \lambda(r)u - \omega(r)v \tag{1a}$$

$$v_t = v_{xx} + \omega(r)u + \lambda(r)v \tag{1b}$$

where $r = (u^2 + v^2)^{1/2}$, u and v are functions of space x and time t, subscripts $_x$ and $_t$ denote partial derivatives, and $\lambda(0)$ and $\omega(0)$ are both strictly positive. The kinetics of (1) have a circular limit cycle of any radius r that is an isolated zero of $\lambda(.)$, which will be stable if and only if $\lambda(.)$ decreases monotonically on a neighbourhood of r. Following many previous authors, I study the system (1) as a prototype for more general reaction–diffusion systems in which the kinetics have a stable limit cycle.

I will consider a number of different functional forms for $\lambda(r)$ and $\omega(r)$, with $\lambda(r) = 0$ having a unique real positive root, at $r = r_L$ say, in each case. Kopell and Howard (1973) showed that in such a case (1) has an essentially unique one-parameter family of periodic plane wave solutions, given by

$$u = \hat{r}\cos[\omega(\hat{r})t \pm \lambda(\hat{r})^{1/2}x] \tag{2a}$$

$$v = \hat{r}\sin[\omega(\hat{r})t \pm \lambda(\hat{r})^{1/2}x] \tag{2b}$$

with $0 < \hat{r} < r_L$. Thus the periodic plane waves are all circular in the u–v plane, and lie inside the limit cycle of the kinetics. Kopell and Howard (1973) also showed that (2) is linearly stable as a solution of (1) if and only if

$$4\lambda(\hat{r})\left[1 + \left(\frac{\omega'(\hat{r})}{\lambda'(\hat{r})}\right)^2\right] + \hat{r}\lambda'(\hat{r}) \leqslant 0. \tag{3}$$

In particular, waves of sufficiently large amplitude are stable, and waves of sufficiently small amplitude are unstable.

I consider the solution of systems of the form (1) on $0 < x < \infty$, $t > 0$, with initial conditions

$$u(x, 0) = v(x, 0) = A\exp(-\xi x) \tag{4}$$

where A and ξ are positive constants, with A small compared to $\lambda(.)$ and $\omega(.)$. I take the boundary conditions to be $u, v \to 0$ as $x \to \infty$, with either $u_x = v_x = 0$ or u and v specified at $x = 0$. In a previous publication (Sherratt 1993a), I showed that in the particular case

$$\lambda(r) = \lambda_0 - r^p \qquad \omega(r) = \omega_0 - r^p \tag{5}$$

where λ_0, ω_0 and p are positive constants, the solution of (1) evolves from (4) into a wave front moving in the positive x direction, leaving periodic plane waves behind it. I derived a relationship for the amplitude of these periodic plane waves as a function of the decay rate ξ and the other parameters. Here I extend this work to other λ–ω systems. In particular I show that when $\lambda(r)$ is a cubic function with $[\omega(r) - \omega(0)]^2$ linear, there is a bifurcation in the amplitude of the periodic plane waves behind the leading wave front as the slope of $[\omega(r) - \omega(0)]^2$ passes through a critical value. My motivation for studying a wider range of λ–ω systems is the ultimate goal of progressing to more general reaction–diffusion systems, which I am only able to study numerically at the moment (Sherratt 1993b, c). An understanding of the breadth of phenomena possible in λ–ω systems is an important first step in this progression.

2. Monotonic $\lambda(r)$ and $\omega(r)$

It is most convenient to analyse (1) using polar coordinates in u–v space, that is $r = (u^2 + v^2)^{1/2}$, $\theta = \tan^{-1}(v/u)$, in terms of which the partial differential equations (1) are

$$r_t = r\lambda(r) + r_{xx} - r\theta_x^2 \tag{6a}$$

$$\theta_t = \omega(r) + \theta_{xx} + 2r_x\theta_x/r. \tag{6b}$$

When $\lambda(.)$ and $\omega(.)$ are given by (5), numerical evidence suggests that the exponentially decaying initial data (4) evolve to transition wave fronts of constant shape and speed in r and θ_x, moving in the positive x direction (Sherratt 1993a). The solutions are essentially independent of A and the boundary conditions at $x = 0$. The steady-state values behind the transition front correspond to a periodic plane wave, and the speed s of the front is given by

$$s = \begin{cases} \xi + \lambda(0)/\xi & 0 < \xi \leqslant \sqrt{\lambda(0)} \\ 2\sqrt{\lambda(0)} & \xi \geqslant \sqrt{\lambda(0)}. \end{cases} \tag{7}$$

This speed is familiar from solutions of the Fisher equation (McKean 1975, Larson 1978, Rothe 1978, Manoranjan and Mitchell 1983), and can be justified intuitively on the basis that (6a) has the same linearization as the Fisher equation at the leading edge of a transition front. Numerical solutions for a number of other forms of $\lambda(.)$ and $\omega(.)$ for which $\lambda(.)$ is monotonically decreasing and $\omega(.)$ is either monotonically increasing or decreasing also exhibit this behaviour of transition wave fronts in r and θ_x, with wave speed given by (7), as illustrated in figure 1. The steady state behind the transition front corresponds to periodic plane waves.

Based on these observations, and following my previous approach (Sherratt 1993a), I look for solutions of (6) of the form $r = \tilde{r}(z)$, $\theta_x = \tilde{\psi}(z)$, where $z = x - st$ and $\tilde{r}(z)$, $\tilde{\psi}(z) \to 0$ as $z \to \infty$. This implies that $r(x, t) = \tilde{r}(x - st)$ and $\theta(x, t) = \tilde{\Psi}(x - st) + \omega(0)t$, where $\tilde{\Psi}(.)$ is an indefinite integral of $\tilde{\psi}(.)$. The functions $\tilde{r}(.)$ and $\tilde{\psi}(.)$ must satisfy a third-order system of ordinary differential equations:

$$\tilde{r}'' + s\tilde{r}' + \tilde{r}\lambda(\tilde{r}) - \tilde{r}\tilde{\psi}^2 = 0 \tag{8a}$$

$$\tilde{\psi}' + (s + 2\tilde{r}'/\tilde{r})\tilde{\psi} + \omega(\tilde{r}) - \omega(0) = 0. \tag{8b}$$

Non-trivial steady states $\tilde{r} = \tilde{r}_s$, $\tilde{\psi} = \tilde{\psi}_s$ of this system have $\tilde{\psi}_s = [\omega(0) - \omega(\tilde{r}_s)]/s$, with $\tilde{r}_s$ a solution of

$$\lambda(\tilde{r}_s) = \left[\frac{\omega(\tilde{r}_s) - \omega(0)}{s}\right]^2. \tag{9}$$

When $\lambda(.)$ is a monotonically decreasing function, with $\omega(.)$ either monotonically increasing or monotonically decreasing, (9) has a unique solution for $\tilde{r}_s$. Therefore, one expects that the steady-state values of r and θ_x behind the transition front are just $\tilde{r}_s$ and $\tilde{\psi}_s$, with the transition front corresponding to a heteroclinic connection in (8) between $\tilde{r} = \tilde{r}_s$, $\tilde{r}' = 0$, $\tilde{\psi} = \tilde{\psi}_s$ and $\tilde{r} = \tilde{r}' = \tilde{\psi} = 0$. I have confirmed this numerically for a number of different functional forms of λ and ω, and an example is illustrated in figure 2.

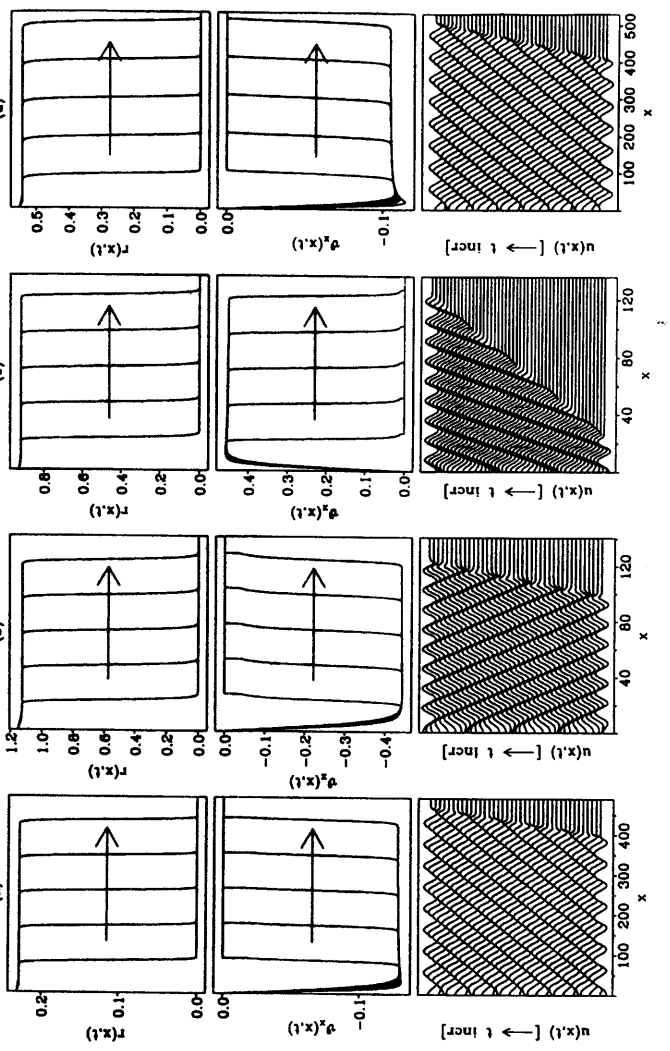

Figure 1. Examples of the solution of (1) subject to (4) for monotonic $\lambda(.)$ and $\omega(.)$. I plot r and θ_x as functions of x at equally spaced times, and u as a function of x at successive times t, with the vertical spacing of solutions proportional to the time interval. In all cases, the solution evolves to transition fronts in r and θ_x, moving with constant shape and speed; the steady state behind the front corresponds to periodic plane waves. The sign of θ_x behind the front is positive or negative according to whether $\omega(.)$ is decreasing or increasing, respectively, and the direction of motion of the periodic plane waves is in the positive or negative direction according to whether $\omega(0)/\omega(\bar{r}_s) - 1$ is positive or negative, respectively. The functional forms for $\lambda(.)$ and $\omega(.)$ are: (*a*) $\lambda(r) = 2 - e^{3r}$, $\omega(r) = e^r$, with $\xi = 4$; (*b*) $\lambda(r) = 2 - r^5$, $\omega(r) = 4 - r^2$, with $\xi = 3$; (*c*) $\lambda(r) = (4 - r^6 e^{2r})/\log(3 + r)$, $\omega(r) = 1 - r^4 e^r$, with $\xi = 2$; (*d*) $\lambda(r) = 1 - 2\tanh r$, $\omega(r) = \log(2 + r)$, with $\xi = 4$. The time intervals between the r and θ_x solutions are approximately (*a*) 44; (*b*) 8.9; (*c*) 6.4; (*d*) 47, and the range of times in the plots of $u(x, t)$ are (*a*) $187 \leqslant t \leqslant 220$; (*b*) $35.6 \leqslant t \leqslant 44.5$; (*c*) $6.4 \leqslant t \leqslant 32$; (*d*) $188 \leqslant t \leqslant 235$. Here and in numerical solutions of the reaction–diffusion equations presented in other figures, equations (1) were solved using the method of lines and Gear's method, and the value of A was 0.1. The solutions are essentially independent of A.

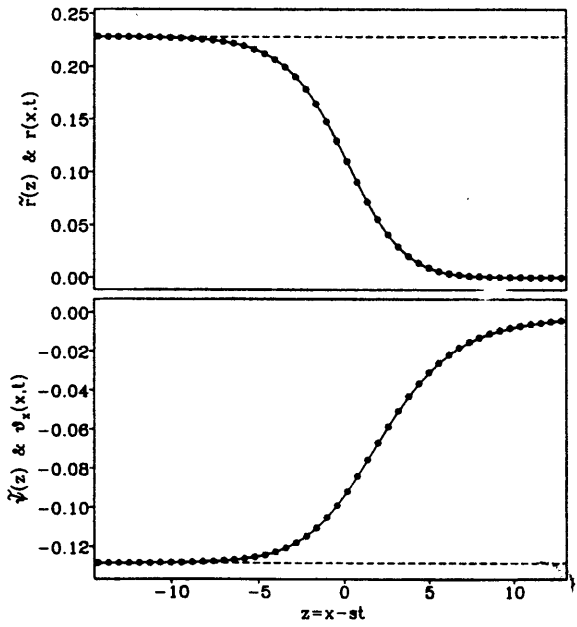

Figure 2. An example of the comparison of the transition waves in r and θ_x in the solution of (1) subject to (4) (——), with the heteroclinic connection in (8) between $\tilde{r} = \tilde{r}' = \tilde{\psi} = 0$ and $\tilde{r} = \tilde{r}_s$, $\tilde{r}' = 0$, $\tilde{\psi} = \tilde{\psi}_s$ (•). The forms for $\lambda(.)$ and $\omega(.)$ are as in figure 1(a), and the comparison is equally good for a variety of other forms for $\lambda(.)$ and $\omega(.)$. The heteroclinic connection was calculated by solving the system (8) numerically as an initial value problem, using a Runge–Kutta–Merson method. The initial value used was $\tilde{r} = \tilde{r}_s - \epsilon e_1$, $\tilde{r}' = -\epsilon e_2$, $\tilde{\psi} = \tilde{\psi}_s - \epsilon e_3$, where $0 < \epsilon \ll 1$, and (e_1, e_2, e_3) is the normalized eigenvector corresponding to the unique positive eigenvalue of (8) at the non-zero steady state. The broken lines indicate the steady-state values $\tilde{r}_s$ and $\tilde{\psi}_s$.

To be specific, I consider in particular detail the case of $\lambda(r) = \lambda_0 - r^p$, $\omega(r) = \omega_0 \pm r^{\alpha p}$, where λ_0, ω_0, p and α are strictly positive parameters. For this system, (9) is

$$R^{2\alpha} + s^2 R - s^2 \lambda_0 = 0 \tag{10}$$

where $R = \tilde{r}_s^p$, and the result (3) implies that the periodic plane wave of amplitude $\tilde{r}_s$ will be linearly stable as a solution of (1) if and only if

$$p \geqslant p_{\text{crit}} = (4/s^2)(R^{2\alpha-1} + \alpha^2 R^{4\alpha-3}). \tag{11}$$

When $p < p_{\text{crit}}$, the periodic plane wave solution $r = \tilde{r}_s$, $\theta = \tilde{\psi}_s x + \omega_0 t$ is unstable. Numerical solutions in this case show a band of periodic plane waves immediately behind the transition front in r, with more irregular oscillations further back (figure 3). It is important to stress, however, that there is not a sudden change in the solutions as p decreases through p_{crit}. Rather, there is a gradual development of irregular oscillations behind a band of regular oscillations, whose thickness decreases as p decreases and the periodic plane waves become gradually more unstable. One striking observation in figure 3, which is also true for the wide range of other parameter sets that I have tried, is that these irregular oscillations have an amplitude which, although it varies, is always less than $r_L = \lambda_0^{1/p}$. The fact that, provided $A < r_L/\sqrt{2}$, $0 \leqslant r(x,t) \leqslant r_L$ for all $x, t > 0$, is implied by the following result:

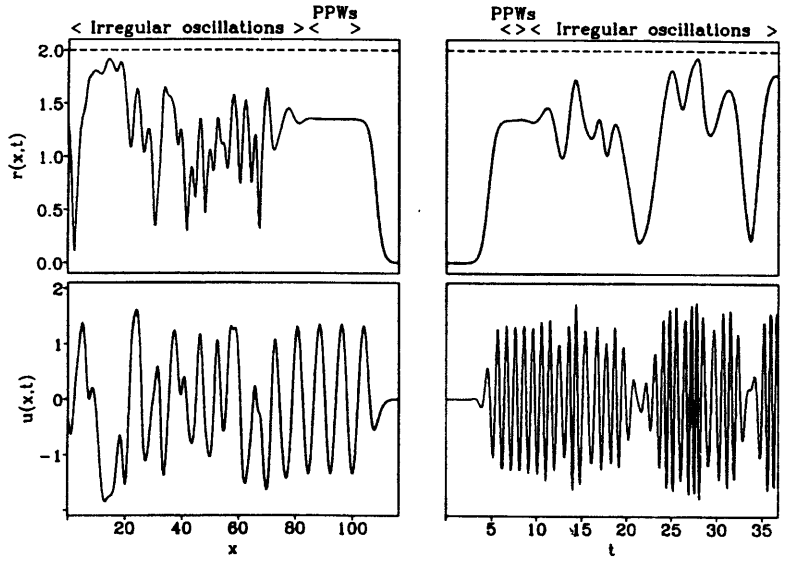

Figure 3. An example of the solution of (1) subject to (4) with $\lambda(r) = \lambda_0 - r^p$ and $\omega(r) = \omega_0 - r^{\alpha p}$ when $p < p_{\text{crit}}$. I plot r and u as functions of x at $t = 37$, and as functions of t at $x = 11$. The amplitude r_L of the limit cycle in the kinetics is denoted by a dashed line. The solution consists of a transition front in r (and θ_x), with periodic plane waves of amplitude $\tilde{r}_s$ immediately behind this transition front. However, these periodic plane waves are unstable as reaction–diffusion solutions, and degenerate further back to give irregular spatiotemporal oscillations. The parameter values are $\lambda_0 = 2$, $\omega_0 = 4$, $p = 1$, $\alpha = 3$, $\xi = 1$.

Consider a λ–ω system (1) with $x \in \mathbb{R}$ and with $r\lambda(r) = 0$ having real positive roots at $r = r_1$ and $r = r_2 > r_1$. If at some time $t = t_0$, $r_1 \leqslant r(x, t_0) \leqslant r_2 \forall x \in \mathbb{R}$, then $\forall t > t_0$, $r_1 \leqslant r(x, t) \leqslant r_2 \forall x \in \mathbb{R}$.

The proof of this result is straightforward. If $r(x, t) > r_2$ for some x and $t > t_0$ then by continuity there must be a previous time $t_1 \geqslant t_0$ at which $r(x, t_1) \leqslant r_2 \forall x$, with some point $x = x^*$ at which $r = r_2$ and $r_t > 0$. Since r has a local maximum at $x = x^*$, $r_{xx} \leqslant 0$, so that $r_t = r\lambda(r) + r_{xx} - r\theta_x^2 = r_{xx} - r_2\theta_x^2 \leqslant -r_2\theta_x^2 \leqslant 0$, which is a contradiction. Similarly $r \geqslant r_1$ for all x and $t > t_0$. The result also holds when the spatial domain is half the real line or an interval of the real line, provided the boundary conditions at the finite boundaries are either u and v fixed (at values such that $r_1^2 \leqslant u^2 + v^2 \leqslant r_2^2$) or $u_x = v_x = 0$.

3. Cubic $\lambda(r)$ and linear $[\omega(r) - \omega(0)]^2$

Since $\lambda(r) > 0$ on $[0, r_L)$ with $\lambda(r_L) = 0$, and $[\omega(r) - \omega(0)]^2 \geqslant 0$ with equality at $r = 0$, (9) will always have at least one root on $(0, r_L]$. However, when $\lambda(.)$ and $\omega(.)$ are not monotonic, there may be more than one root, although there will always be an odd number of roots (counting roots by multiplicity). I consider here one class of functional forms for which there are either one or three roots, depending on parameters. The particular functional forms I consider do not have any special significance. Rather, I use them to illustrate the type of behaviour that can evolve from initial conditions of the form (4) in a λ–ω system for which (9) has more than one root.

The system I consider is

$$\lambda(r) = k - (r - b - a)(r - b)(r - b + a) \qquad \omega(r) = \Omega - cr^{1/2} \tag{12}$$

subject to the following parameter restrictions: (i) $b > a/\sqrt{3}$; (ii) $k > 2a^3/3^{3/2}$; (iii) $k < a^2 b$. The form of $\lambda(r)$ is illustrated in figure 4. Condition (ii) ensures that $\lambda(r) = 0$ has a single real root, while condition (i) ensures that both turning points occur at positive values of r. The right-hand side of (9) is the linear function $(c^2/s^2)r$, which can intersect $\lambda(r)$ at either one or three points. Now the maximum positive slope of $\lambda(r)$ occurs between the turning points, at $r = b$, and condition (iii) implies that the slope of $\lambda(r)$ at this point is greater than that of the line joining $(b, \lambda(b))$ and $(0, 0)$. Therefore, as c varies, (9) will have three real positive roots for $c_2 \geqslant c \geqslant c_1 > 0$, with one real positive root for $c > c_2$ and $c < c_1$. Here c_1 and c_2 are critical values that depend on s, k, b and a, and that can in principle be determined analytically. The variation with c of the roots of (9) is illustrated in figure 4.

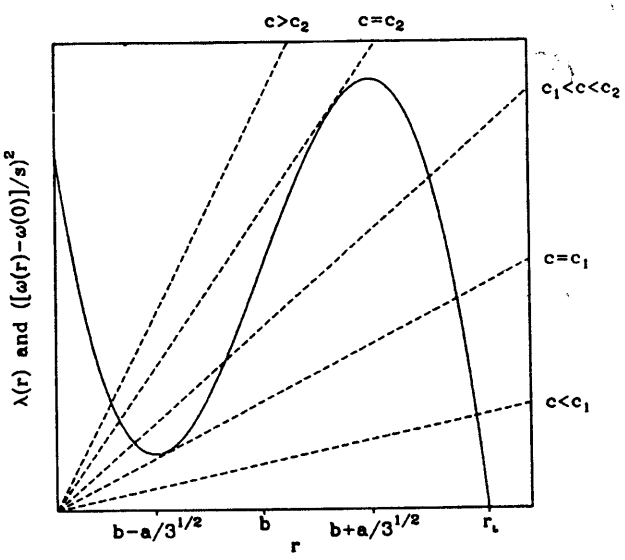

Figure 4. An illustration of the qualitative forms of $\lambda(r)$ (full curve) and $[(\omega(r) - \omega(0))/s]^2$ (broken curve) given by (12). The latter function is shown for a variety of values of the parameter c. Intersections of these curves are roots of (9), and the number of roots changes from 1 to 3, and then back to 1 again, as c increases.

I begin by considering the nature of these roots as steady states of the third-order system of ordinary differential equations (8). Straightforward linearization shows that at a steady state $(\tilde{r}_s, 0, \tilde{\psi}_s)$, where $\tilde{r}_s$ is a root of (9), the eigenvalues μ satisfy

$$\mu^3 + 2s\mu^2 + [s^2 + 4\lambda(r_s) + r_s\lambda'(r_s)]\mu + [sr_s(\lambda'(r_s) - c^2/s^2)] = 0.$$

If $\lambda'(r_s) > c^2/s^2$, then the Routh–Hurwitz conditions imply that all the eigenvalues have negative real part, so that the steady state is stable. When there are three roots for (9), this is the case for the middle root. Conversely, if $\lambda'(r_s) < c^2/s^2$, Descarte's rule of signs implies that exactly one of the eigenvalues is real and positive, so that the steady state is

unstable. Since the sum of the three eigenvalues is negative, the other two must either be real and negative or a complex conjugate pair with negative real part. This is the case when there is a single root of (9), and for the smallest and largest roots when there are three.

A final preliminary observation concerns the stability as solutions of (1) of the periodic plane waves whose amplitudes are roots of (9). When there are three roots, the slope of λ is positive at the middle one; therefore (3) implies that the corresponding periodic plane waves are linearly unstable. The waves corresponding to the other two roots can be stable or unstable, depending on the parameters; however, it is straightforward to determine the stability numerically, using (3), for any given set of parameters.

A typical example of the variation with c of the solutions of (11) with (12) subject to (4) is illustrated in figure 5. For $c < c_1$, there is a single root of (9), and the solution of the reaction–diffusion system again has the form of an advancing wave front, with periodic plane waves behind this front (figure 5(*a*)). The amplitude of the waves is equal to the root of (9). For the example shown in figure 5(*a*), these periodic plane waves are stable as solutions of (1); however, for other parameters they are unstable, and then the waves degenerate into more irregular oscillations further back from the leading front, as discussed previously. For c just below c_1 there is a band of smaller amplitude oscillations immediately behind the leading front; this band appears to have constant width (figure 5(*b*)).

As c increases through c_1, the solution bifurcates and the amplitude of the periodic plane waves behind the advancing front changes to the smallest root of (9) (figure 5(*c*)). Again, if these periodic waves are unstable as solutions of (1), they degenerate into more irregular oscillations further back. This will always be the case for c just above c_1, since $\lambda'(r_s)$ will then be positive. For the parameter values used in figure 5(*c*), the periodic plane waves with amplitude the smallest root of (9) are in fact unstable as solutions of (9). However, they are only just unstable, and thus the solutions consist of a wide band of periodic plane waves, with larger amplitude oscillations much further back.

As c increases above c_1, the solution changes gradually as the smallest root of (9) varies, and as the stability of the corresponding periodic plane waves varies. As c increases through c_2, so that the number of roots of (9) returns to one, this gradual variation continues (figures 5(*d*) and 5(*e*)), and there is no sudden change in the reaction–diffusion solution.

In order to explain these results, I return to the ordinary differential equations (8) governing travelling fronts in r and θ_x. When there is a unique root of (9), I have shown above that the corresponding steady state has one real, positive eigenvalue, with the other eigenvalues having negative real parts. Therefore there are exactly two trajectories originating from this steady state in $\tilde{r}$–$\tilde{r}'$–$\tilde{\psi}$ phase space; the only other steady state is (0, 0, 0). Numerical phase portraits strongly suggest that one of the trajectories originating from $(\tilde{r}_s, 0, \tilde{\psi}_s)$ terminates at (0, 0, 0) (figure 6(*a*)), and it is to this heteroclinic connection that the solutions of (9) evolve.

When there are three roots of (9), I have shown that the steady state of (8) corresponding to the middle root is stable, while those corresponding to the smallest and largest roots are unstable, with exactly two trajectories originating from each steady state. What are the connections between these steady states? Numerical evidence suggests that there are heteroclinic connections between the steady state corresponding to the middle root of (9) and those corresponding to both of the other roots, and that there is also a connection between the steady state corresponding to the smallest root of (9) and (0, 0, 0). However, it appears that there is no connection between the largest root of (9) and (0, 0, 0) (figures 6(*b*) and 6(*c*)). I have been unable to prove that such a connection does not exist but I now establish a partial result, that there does not exist a connection between these steady states that is monotonically decreasing in r.

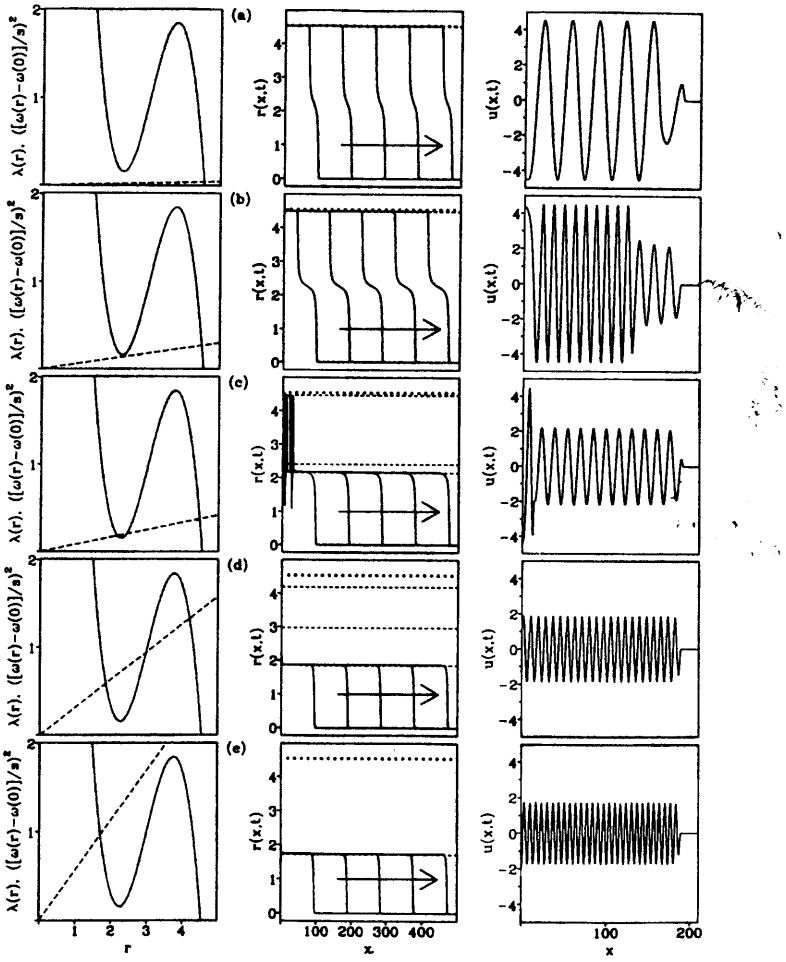

Figure 5. An example of the variation with c of the solutions of (1) subject to (4), when $\lambda(.)$ and $\omega(.)$ are given by (12). The parameter values are $k = 1$, $b = 3$, $a = 1.3$, $\Omega = 1$, $\xi = 3$ and (*a*) $c = 1$ (*b*) $c = 2.7$ (*c*) $c = 3.1$ (*d*) $c = 6$ (*e*) $c = 8$. For each value of c, there are three figure parts. In the first part, I plot the left-hand side (full curve) and right-hand side (broken curve) of (9) against r. The left-hand side is independent of c. In the second part, I plot the solution amplitude r as a function of x at equally spaced times. The time interval is approximately 8.5 and is the same for each c. The values of r that are roots of (9) are denoted by broken horizontal lines, and the amplitude r_L of the limit cycle in the kinetics is denoted by a dotted line. In the third part, I plot the solution for u as a function of space at $t \approx 17$. The interpretation of the variation in solution form with c is discussed in detail in the main body of the paper.

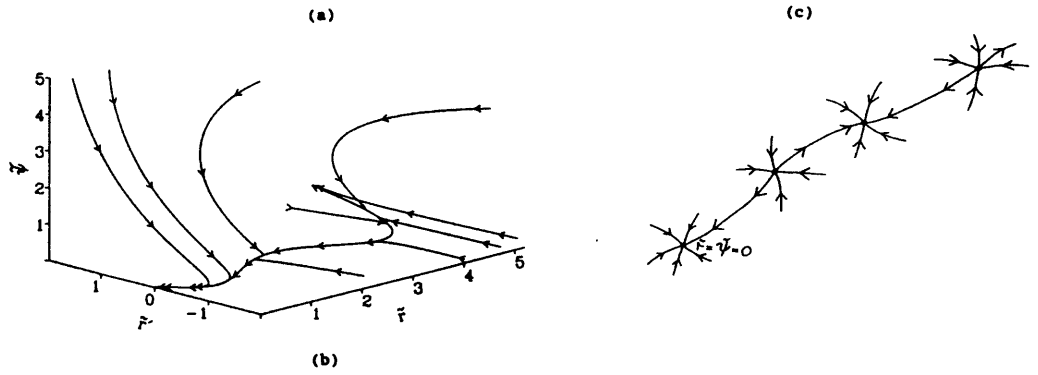

Figure 6. (*a*) The phase portrait of the system (8) for the parameter values used in figure 5(*a*), so that $c < c_1$. There is a unique non-zero steady state (•), and there appears to be a heteroclinic connection between this steady state and $\tilde{r} = \tilde{r}' = \tilde{\psi} = 0$. (*b*) The phase portrait of the system (8) for the parameter values used in figure 5(*d*), so that $c_1 < c < c_2$. There are three non-zero steady states (denoted by •). The apparent connections between these steady states are illustrated schematically in (*c*).

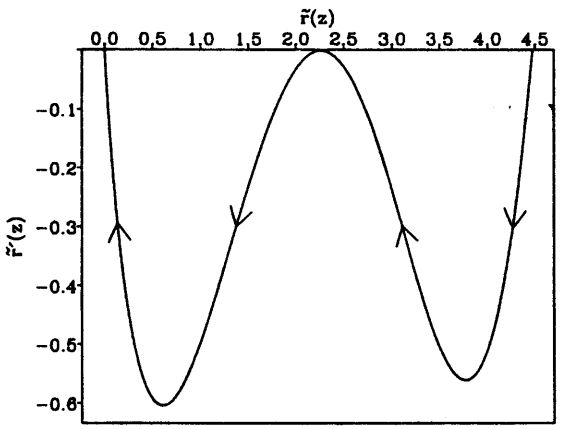

Figure 7. A projection onto the $\tilde{\psi} = 0$ plane of the heteroclinic connection between the unique non-zero steady state and the origin in (8), for the parameter values used in figure 5(*b*). The third variable $\tilde{\psi}$ decreases monotonically along this trajectory. The heteroclinic connection was calculated as described in the legend to figure 2. This figure illustrates that the band of small amplitude oscillations is simply a facet of the shape of the heteroclinic connection, along which $\tilde{r}'$ becomes very small (but is still strictly positive) at $\tilde{r} \approx 2.2$.

To prove this, denote $\tilde{r}' = w$, so that the system (8) is

$$\tilde{r}' = w \tag{13a}$$

$$w' = -sw - \tilde{r}\lambda(\tilde{r}) + \tilde{r}\tilde{\psi}^2 \tag{13b}$$

$$\tilde{\psi}' = -s\tilde{\psi} - (2w/\tilde{r})\tilde{\psi} + c\tilde{r}^{1/2}. \tag{13c}$$

Let $\tilde{r}_1$ be some value less than the middle root of (9), and greater than both the smallest root of (9) and the position of the local minimum of $\lambda(.)$. There is then a unique value of $\tilde{r}$, $\tilde{r}_2$ say, on $(\tilde{r}_1, r_L)$, satisfying $\lambda(\tilde{r}_2) = \lambda(\tilde{r}_1)$, and the largest two roots of (9) both lie in $(\tilde{r}_1, \tilde{r}_2)$. Consider the portion $\tilde{r} > \tilde{r}_1$, $w < 0$ of the plane $\tilde{\psi} = \sqrt{\lambda(\tilde{r}_1)}$. Then

$$\tilde{\psi} > -s\sqrt{\lambda(\tilde{r}_1)} + c\,\tilde{r}_1^{1/2} > 0 \tag{14}$$

since the right-hand side of (9) is greater than the left-hand side at $\tilde{r}_1$.

Now restrict attention to $\tilde{\psi} > \sqrt{\lambda(\tilde{r}_1)}$ and $\tilde{r}_1 < \tilde{r} < \tilde{r}_2$, and let $\Lambda(\tilde{r})$ be a smooth function satisfying $\Lambda(\tilde{r}) > \tilde{r}_2[\lambda(\tilde{r}) - \lambda(\tilde{r}_1)]$ on $\tilde{r}_1 < \tilde{r} < \tilde{r}_2$, with $\Lambda(\tilde{r}_1) = \Lambda(\tilde{r}_2) = 0$, and $\Lambda'(\tilde{r}_1) > 0$, $\Lambda'(\tilde{r}) < \Lambda'(\tilde{r}_1)$ on $(\tilde{r}_1, \tilde{r}_2]$. It is clear that such a function exists. Then

$$w' = -sw - \tilde{r}\lambda(\tilde{r}) + \tilde{r}\tilde{\psi}^2 > -sw - \tilde{r}[\lambda(\tilde{r}) - \lambda(\tilde{r}_1)] > -sw - \tilde{r}_2[\lambda(\tilde{r}) - \lambda(r_1)] > -sw - \Lambda(\tilde{r}). \tag{15}$$

Consider now the second-order system given by (13*a*) and $w' = -sw - \Lambda(\tilde{r})$. This system has steady states at $\tilde{r} = \tilde{r}_1$, $w = 0$ and $\tilde{r} = \tilde{r}_2$, $w = 0$, and it is a standard result that there is a heteroclinic connection between these two steady states (Kolmogoroff *et al* 1937). This connection consists of a trajectory originating from $(\tilde{r}_2, 0)$ and terminating at $(\tilde{r}_1, 0)$; it remains in the half plane $w < 0$, and thus $\tilde{r}$ decreases monotonically along it. I denote this trajectory by $w = W(\tilde{r})$.

Returning to the third-order system (13), consider the set, $\mathcal{S}$ say, with $\tilde{r}_1 < \tilde{r} < \tilde{r}_2$ and $\tilde{\psi} > \sqrt{\lambda(\tilde{r}_1)}$, bounded by the surface $w = W(\tilde{r})$, and the planes $w = 0$ and $\tilde{\psi} = \sqrt{\lambda(\tilde{r}_1)}$. The steady states corresponding to the middle and largest root of (9) lie on the $w = 0$ portion of $\partial\mathcal{S}$, while $(0, 0, 0)$ lies outside $\mathcal{S}$. Moreover, the inequalities (14) and (15) imply that all trajectories that leave $\mathcal{S}$ do so through the $w = 0$ portion of $\partial\mathcal{S}$, entering the $w > 0$ half space. Therefore if a trajectory leaving the steady state corresponding to the largest root of (9) terminates at $(0, 0, 0)$, it must have $\tilde{r}' > 0$ at some point along its length, which is the required result. As I have already mentioned, numerical evidence suggests that in fact there is no such trajectory.

I return now to the numerical solutions of the partial differential equations, illustrated in figure 5 and discussed above. The observed bifurcation in these solutions at $c = c_1$ admits a simple explanation in terms of the heteroclinic connections in the phase space of (8). As c increases through c_1, the connection between the origin and the steady state corresponding to the largest root of (9) disappears, and a connection between the origin and the steady state corresponding to the smallest root of (9) appears. This change in connections mirrors exactly the change in the transition fronts in r and θ_x observed in solutions of (1). When c is just below c_1, the observed band of small amplitude oscillations immediately behind the transition front in r (as in figure 5(*b*)) is simply a facet of the shape of the heteroclinic connection, along which $\tilde{r}'$ comes close to zero (figure 7).

References

Agladze K I, Krinsky V I, Pertsov A M 1984 Chaos in the non-stirred Belousov Zhabotinsky reaction is induced by interaction of waves and stationary dissipative structures *Nature* **308** 834–5

Cope D 1980 Stability of limit cycle solutions of reaction–diffusion equations *SIAM J. Appl. Math.* **38** 457–79

Courtemanche M and Winfree A T 1991 Re-entrant rotating waves in a Beeler–Reuter based model of two-dimensional cardiac electrical activity *Int. J. Bifurc. Chaos* **1** 431–44

Ermentrout G B 1980 Small amplitude stable wavetrains in reaction–diffusion systems *Lect. Notes Pure Appl. Math.* **54** 217–28

Hagan P S 1982 Spiral waves in reaction–diffusion equations *SIAM J. Appl. Math.* **42** 762–86

Kapitula T M 1991 Stability of weak shocks in λ–ω systems *Indiana Univ. Math. J.* **40** 1193–219

Kolmogoroff A, Petovsky I and Piscounoff N 1937 Etude de l'équation de la diffusion avec croissance de la quantité de matière et son application à un problème biologique *Moscow Univ. Bull. Math.* **1** 1–25 (An English translation of the relevant part of this paper is given in chapter 7 of Oliveira-Pinto F and Conolly B W 1982 *Applicable Mathematics of Non-physical Phenomena* (New York: Wiley)

Kopell N and Howard L N 1973 Plane wave solutions to reaction–diffusion equations *Stud. Appl. Math.* **52** 291–328

Kuramoto Y 1978 Diffusion-induced chaos in reaction systems *Prog. Theor. Phys. Suppl.* **64** 346–67

Larson D A 1978 Transient bounds and time asymptotic behaviour of solutions of nonlinear equations of Fisher type *SIAM J. Appl. Math.* **34** 93–103

Maginu K 1981 Stability of periodic travelling wave solutions with large spatial periods in reaction–diffusion systems *J. Diff. Eqns.* **39** 73–99

Manoranjan V S and Mitchell A R 1983 A numerical study of the Belousov–Zhabotinskii reaction using Galerkin finite element methods *J. Math. Biol.* **16** 251–60

McKean H P 1975 Application of Brownian motion to the equation of Kolmogorov–Petrovskii–Piskunov *Commun. Pure Appl. Math.* **28** 323–31

Rothe F 1978 Convergence to travelling fronts in semilinear parabolic equations *Proc. R. Soc.* A **80** 213–34

Rovinsky A B 1987 Twinkling patterns and diffusion-induced chaos in a model of the Belousov–Zhabotinsky chemical medium *J. Phys. Chem.* **91** 5113–8

Schneider K R 1983 A note on the existence of periodic travelling wave solutions with large periods in generalised reaction–diffusion systems *Zeitschrift Ang. Math. Phys.* **34** 236–40

Sherratt J A 1993a On the evolution of periodic plane waves in reaction–diffusion systems of λ–ω type. Submitted

—— 1993b Chaos induced by travelling fronts in reaction–diffusion equations. Submitted.

—— 1993c Transition waves that leave behind regular or chaotic spatiotemporal oscillations in a system of three reaction–diffusion equations *Int. J. Bifurc. Chaos* in press

Tyson J J and Murray J D 1989 Cyclic AMP waves during aggregation of *Dictyostelium* amoebae *Development* **106** 421–6

Winfree A T and Strogatz S H 1983a Singular filaments organize chemical waves in three dimensions. I. Geometrically simple waves *Physica* D **8** 35–49

—— 1983b Singular filaments organize chemical waves in three dimensions. II. Twisted waves *Physica* D **9** 65–80

—— 1983c Singular filaments organize chemical waves in three dimensions. III. Knotted waves *Physica* D **9** 333–45

—— 1984 Singular filaments organize chemical waves in three dimensions. IV. Wave taxonomy *Physica* D **13** 221–33